Fat Suppression for UTE Imaging Using a Novel Soft-Hard Composite RF Pulse

Ya-Jun Ma[1], **Saeed Jerban**[1], **Hyungseok Jang**[1], **Eric Y Chang**[2,1], **Jiang Du**[1]

[1]Department of Radiology, University of California, San Diego, CA

[2]Radiology Service, VA San Diego Healthcare System, San Diego, CA

Abstract

Purpose: To design a soft-hard composite pulse for fat-suppression and water-excitation in ultrashort echo time (UTE) imaging with minimal short T_2 signal attenuation.

Methods: The composite pulse contains a narrow bandwidth soft pulse centered on the fat peak with a small negative flip angle ($-\alpha$) and a short rectangular pulse with a small positive flip angle (α). The fat magnetization experiences both tipping-down and -back with an identical flip angle and thus returns to the equilibrium state, leaving only the excited water magnetization. Bloch simulations, as well as knee, tibia, and ankle UTE imaging studies, were performed to investigate the effectiveness of fat-suppression and corresponding water signal attenuation. Conventional fat saturation (FatSat) module was used for comparison. Signal suppression ratio (SSR), defined as the ratio of signal difference between non-fat-suppression and fat-suppression images over the non-fat-suppression signal, was introduced to evaluate the efficiency of the composite pulse.

Results: Numerical simulations demonstrate the soft-hard pulse has little saturation effect on short T_2 water signals. Knee, tibia, and ankle UTE imaging results suggest that comparable fat-suppression can be achieved with the soft-hard pulse and the FatSat module. However, much less water saturation is induced by the soft-hard pulse especially for short T_2 tissues, with SSRs reduced from 71.8±6.9% to 5.8±4.4% for meniscus, from 68.7±5.5% to 7.7±7.6% for bone, and from 62.9±12.0% to 4.8±3.2% for the Achilles tendon.

Conclusion: The soft-hard composite pulse can suppress fat signals in UTE imaging with little signal attenuation on short T_2 tissues.

INTRODUCTION

Ultrashort echo time (UTE) sequences with echo times less than 100μs can detect fast decaying signals and provide a much higher signal to noise ratio (SNR) for short T_2 tissues than conventional clinical gradient recalled echo (GRE)-type sequences with much longer

Corresponding Author: Jiang Du, Ph.D., jiangdu@ucsd.edu, University of California, San Diego, Department of Radiology, 200 West Arbor Drive, San Diego, CA 92103-8226, Phone: (619) 471-0519, Fax: (619) 471-0503.

echo times (1). In the past decade, these UTE sequences have been widely investigated for both morphological and quantitative imaging of short T_2 tissues including calcified cartilage, menisci, tendons, ligaments, bone, and myelin (2–7).

Fat suppression is very important for UTE imaging of musculoskeletal (MSK) tissues (8–10). This is because UTE imaging tends to show a high fat signal, due to fat's high proton density and short T_1 value, which lead to low contrast for short T_2 tissues. Additionally, UTE imaging of short T_2 tissues often suffers from fat contamination due to partial volume effect, as well as from off-resonance artifacts induced by non-Cartesian UTE acquisition. Thus, for both high contrast morphological imaging and accurate quantitative imaging of short T_2 tissues, it is crucial to incorporate fat suppression techniques with UTE imaging.

The most commonly used approach for fat suppression in clinical practice is the chemical shift-based fat saturation (also called FatSat module), which includes a spectrally selective RF pulse followed by a gradient spoiler. However, the FatSat module is not well-suited for short T_2 imaging due to its strong direct attenuation of the broad frequency spectrum of short T_2 tissues (11). Furthermore, a relatively large saturation flip angle (i.e., no less than 90°) is used in the FatSat module, which also leads to indirect signal attenuation induced by the magnetization transfer (MT) effects, especially for the collagen-rich tissues (12). Other techniques, such as the long T_2 suppression RF pulse (13,14) or the inversion recovery preparations (15–18), can generate high contrast in morphological UTE imaging of short T_2 tissues. However, they can only be conditionally useful for quantitative UTE imaging because the long T_1 components in short T_2 tissues are also partially suppressed by these techniques (19,20). Moreover, fat separation-based methods, such as the single-point Dixon, Iterative Decomposition of water and fat with Echo Asymmetry and Least-squares estimation (IDEAL), and UTE spectroscopic imaging (UTESI), can be incorporated in both morphological and quantitative UTE imaging (21–23). However, they require longer acquisition time and data post-processing.

In this study, we proposed a new fat suppression RF pulse for UTE imaging of short T_2 tissues with well-preserved short T_2 signals using a soft-hard composite pulse. Bloch simulations were performed to investigate its signal attenuation effects on both short and long T_2 tissues, which were then compared with both non-fat suppression excitation and the conventional FatSat technique. Then, *in vivo* knee and tibia, as well as *ex vivo* ankle UTE imaging studies were performed to evaluate the effectiveness of fat suppression and to investigate the corresponding short T_2 signal attenuation for both the proposed soft-hard composite pulse and the conventional FatSat module.

METHODS

Soft-hard composite pulse design

Features of the newly designed soft-hard composite pulse and the conventional FatSat module are both shown in Figure 1. The proposed fat suppression pulse or water excitation pulse consists of two RF pulses: one soft pulse (minimum-phase Shinnar-Le Roux (mip-SLR) design with a duration of 4.4ms and spectral bandwidth of 500Hz) and one hard pulse (Figure 1A) (24). The soft pulse centers on the fat peak with a narrow bandwidth. It is used

to flip only the fat magnetization and is followed by a short hard pulse with a same flip angle as the soft pulse, which flips both water and fat magnetizations in the opposite direction. Since the fat magnetization experiences both tipping down and tipping back with this identical flip angle, most of the fat magnetization returns to the equilibrium state. Subsequently, most of the fat signals are not received by the subsequent UTE acquisitions. In addition, the soft pulse has been designed with a narrow bandwidth and with a pulse duration of several milliseconds; thus, the RF power of the soft pulse is relatively low. The soft pulse excitation is therefore expected to have little saturation effect on the water magnetizations. This makes it possible for the water signals to be effectively excited by the following hard pulse.

The conventional FatSat technique consists of a saturation pulse (mip-SLR design with a duration of 8ms and bandwidth of 500Hz) centered on the fat peak with a flip angle no less than 90°, followed by a gradient spoiler to crush all the excited transverse magnetizations (Figure 1B). Then, a short hard pulse is employed for signal excitation.

Typically, the flip angle of the soft pulse (the same as the excitation flip angle) in the soft-hard composite pulse is much lower than 90° for UTE imaging. Therefore, both direct and indirect saturations (i.e., MT effect) of the water signals produced by the soft pulse in the proposed soft-hard composite pulse are much less than the water signal attenuations induced by the FatSat module.

Numerical Simulations

Bloch simulation was carried out to compare the excitations of a single hard pulse, the proposed soft-hard composite pulse, and the conventional FatSat module for both short and long T_2 imaging with tissue T_2s of 0.3, 0.5, 1, 2, 5, and 20 ms. The T_2 of fat was 20ms. The excitation flip angle was set to 10° for all three RF pulses in simulation; the other parameters were as follows: 1) the single hard pulse: duration was 50μs; 2) the soft-hard composite pulse: mip-SLR design, 4.4ms, bandwidth of 500Hz, and center frequency of –440Hz (i.e., off-resonance frequency of fat at 3T); hard pulse duration was 50μs; 3) the GE product FatSat module: mip-SLR design, 8ms, bandwidth of 500Hz, center frequency of –440Hz, and flip angle of 90°; the spoiler gradient area was large enough to keep the dephasing in a single voxel no less than 4π; the duration of hard pulse excitation was 50 μs.

Numerical simulations for UTE acquisitions were also performed to compare the signal intensities using excitations of the single hard pulse, the proposed soft-hard composite pulse, and the FatSat module. Identical pulse shapes, as above, were employed in this simulation; other sequence parameters were as follows: TR=50ms, nominal TE=20μs, and excitation flip angles ranged from 0° to 50°. A constant T_1 value of 800 ms and variable T_2 values of 0.3, 0.5, 1, 2, 5, and 20 ms were used for simulation. The nominal TE is defined as the time between the end of the hard pulse and the k-space center.

UTE Imaging

To compare UTE imaging with and without fat suppression, *in vivo* knee and tibia imaging, as well as *ex vivo* ankle imaging, was performed on a 3T whole body scanner (GE Healthcare Technologies, Milwaukee, WI). An 8-channel transmit/receive knee coil was

used for both RF transmission and signal reception. A 3D UTE-Cones sequence was used for both short and long T_2 tissue imaging with unique k-space trajectories that sampled data along evenly spaced twisting paths in the shape of multiple cones (17,18). Data sampling started at the center of k-space as soon as possible after the RF excitation with a minimal nominal TE of 32μs.

Fat suppression was carried out using both the proposed soft-hard composite pulse and the GE product FatSat module. The single hard pulse excitation UTE imaging without fat suppression was also employed for comparison. All the RF pulse shapes are identical to the pulses used in the simulation section. The following UTE imaging sequences were repeated using the above three excitation pulses, respectively. Five healthy volunteers (22–35 years old) were recruited for knee joint imaging; the sequence parameters of 3D UTE-Cones were as follows: field of view (FOV)=15×15×9.6 cm^3, acquisition matrix=256×256×32, TE=32μs, flip angle=5°, TR=20ms, and scan time=3min36s. Six healthy volunteers (22–35 years old) were recruited for tibia imaging; the sequence parameters of 3D UTE-Cones were as follows: FOV=12×12×16cm^3, matrix=192×192×32, TE=32μs, flip angle=5°, TR=20ms, and scan time=2min45s. Five healthy volunteers (28–84 years old) were recruited for ankle imaging; the parameters of UTE-Cones imaging were as follows: FOV=11×11×6cm^3, matrix=256×256×30, TE=32μs, flip angle=5°, TR=20ms, and scan time=3min22s. Informed consent was obtained from all subjects in accordance with the guidelines of the institutional review board.

Data Analysis

To evaluate both the fat suppression and the water attenuation for the proposed soft-hard composite pulse and the conventional FatSat module, a signal suppression ratio (SSR, unit in percentage), defined as the fraction of the subtracted image between non-fat suppression image and fat suppression image by the non-fat suppression image, was used. A higher SSR value corresponded to better fat suppression or a stronger water attenuation induced by the fat suppression technique employed. Both the pixel-wised SSR maps and region of interest (ROI)-based signal mean and standard deviation values within all tissues were used for comparison. All analysis algorithms were written in Matlab 2017b (The MathWorks Inc., Natick, MA, USA).

RESULTS

Numerical simulation results of the excitation profiles or spectrums for the single hard pulse, the proposed soft-hard composite pulse and the conventional FatSat module are shown in Figure 2. As can be seen from the transverse magnetization (i.e. M_{xy}) profiles in Figures 2A–F, both the soft-hard and the FatSat pulses were able to null the fat signals at −440Hz. However, the signal nulling bandwidth of the soft-hard pulse was narrower than the FatSat pulse, and two side lobes appeared in both sides of the fat peak. This was induced by the off-resonance excitation during the soft pulse, when the spin had a different on-resonance frequency than the fat center frequency. However, when tissue T_2 was getting shorter, the profiles approached those of the standard single hard pulses. On the other hand, though there were larger side lobes in the excitation of fatty tissues, they had little effect on the water

peak, due to the narrower water spectrum. Consequently, the proposed soft-hard composite pulse had very little effect on both short and long T_2 water signals and, therefore, generated similar water excitations as the single hard pulse. The FatSat module had a better fat suppression than the soft-hard composite pulse, especially for the tissue with a broad fat spectrum. In comparison, the high flip angle saturation pulse used in the FatSat module led to a strong direct saturation on the broad spectrum short T_2 water signals. Thus, fewer short T_2 signals were excited compared with those generated by the single hard pulse or the soft-hard pulse.

As can be seen from Figures 2G–L, the longitudinal magnetization (i.e., M_z) profiles generated by the soft-hard pulse is very close to the single hard pulse, which confirms that the soft pulse has little effect on water signals. In contrast, the reduced M_z profiles of the FatSat module compared with those in both excitations of the single hard pulse and the soft-hard pulse demonstrate the strong direct attenuations of the short T_2 signals by the FatSat module.

Simulated UTE imaging results are shown in Figure 3. As evidenced by the Mxy signal curves, higher flip angles demonstrate less effective excitations compared with the single hard pulse excitation. Stronger signal attenuation is induced by the soft pulse with a higher flip angle. When the excitation flip angles are less than $10°$, the proposed soft-hard pulse can get similar signal intensities as the single hard pulse for both short and long T_2 tissues. In comparison, the derived signal curves of the FatSat module are much lower than those of the single hard pulse and soft-hard pulse due to the large direct saturations.

Figure 4 shows the *in vivo* knee UTE-Cones imaging results from a 24-year-old volunteer. The first three rows are the grayscale images acquired with the single hard pulse, the proposed soft-hard water excitation pulse, and the conventional FatSat module respectively. The last two rows show the SSR colormaps for the two fat suppression methods, respectively. The UTE-Cones images with the excitations of the proposed soft-hard pulse and the product FatSat module both demonstrate good fat suppression and much better image contrast than the non-fat suppression images. The UTE-Cones images with the excitations of a single hard pulse and the soft-hard pulse are displayed with the same value range (i.e., [0, 500]) because of their similar signal intensity levels. In contrast, the FatSat UTE-Cones images are displayed with a much narrower value range (i.e., [0, 200]) due to their lower maximum signal intensities, which were induced by the strong water attenuations (including both direct saturation and MT effect) of the FatSat module. The short T_2 tissues, such as menisci, patellar tendon, and posterior cruciate ligament (PCL) (indicated by arrows), in the UTE-Cones images with the soft-hard pulse excitation show much better preserved signal intensities than those in the FatSat UTE-Cones images. The SSR maps also suggest that there were nearly no signal attenuations for either short or long T_2 tissues when using the proposed soft-hard pulse for excitation. In comparison, there were strong attenuations for the water signals in the FatSat UTE-Cones images, especially for the short T_2 tissues. Similar to the simulation results, the fat suppression technique using the soft-hard pulse was less effective and more spatially inhomogeneous than the FatSat module. This is due to the narrow nulling bandwidth and the additional side lobes of the soft-hard pulse, which induce increased sensitivity to the B_0 inhomogeneity.

Figure 5 shows *in vivo* tibial UTE-Cones imaging results from a 35-year-old volunteer. Like the above knee imaging, the UTE-Cones images with the proposed soft-hard composite pulse excitation show excellent image contrast and well-preserved cortical bone and muscle signals. In comparison, most of the short T_2 signals (i.e., cortical bone and coil elements) are lost in the FatSat UTE-Cones images due to the strong saturation effect of the FatSat module. *Ex vivo* ankle UTE-Cones imaging results from three donors are also shown in Supporting Information Figure S1. Much better SNR and higher contrast of short T_2 tendon signals can be seen in the UTE-Cones images with the soft-hard excitation in comparison to the FatSat UTE-Cones images.

Supporting Information Table S1 summarizes the SSR values for all tissues studied in this work. Both short and long T_2 tissues show much decreased SSRs for the proposed soft-hard pulse compared with those of the FatSat module, demonstrating the proposed excitation pulse's higher excitation efficiency. A slightly lower SSR value was observed for marrow fat with the proposed soft-hard pulse. This is due to the narrower signal nulling bandwidth of the proposed pulse compared with the conventional FatSat module. The results also show relatively high SSR values for the patellar tendon and ACL with the soft-hard pulse, which may be caused by partial volume and fat contamination in the ROIs of patellar tendon and ACL.

Discussion

We have demonstrated in this study that the proposed soft-hard composite pulse is potentially useful for fat suppression in UTE imaging of short T_2 tissues. Numerical simulations show that the proposed soft-hard composite pulse has much lower signal attenuation on water imaging than the conventional FatSat module. *In vivo* knee and tibia, as well as *ex vivo* ankle UTE imaging, demonstrated well-performed fat suppression for the soft-hard pulse excitation. Besides, both the short and long T_2 tissue signals were much better preserved with the soft-hard composite pulse excitation than with the FatSat module for fat suppression. Significantly higher SSRs were achieved with the composite pulse, especially for short T_2 tissues. Such efficient fat signal suppression may improve MRI-based bone assessments (25–27) and reduce the need for extensive scans for sophisticated multicomponent signal analysis (28).

The proposed soft-hard composite pulse can preserve the short T_2 signals while suppressing the fat components, thus providing much higher contrast for short T_2 tissues than the non-fat suppressed images. The soft-hard pulse is relatively sensitive to the B_0 field inhomogeneity due to the narrow bandwidth of the soft pulse. There are also substantial side lobes in the soft-hard pulse excitation that may cause the fat signal to increase in some situations (e.g., in the case where the side lobe locates at the fat peak due to the B_0 inhomogeneity). We can find slightly increased fat signals in some regions with strong B_0 inhomogeneities (e.g., the air-tissue boundary in the middle right of Figure 4D). This phenomenon may occur when the B_0 shift is larger than half of the fat frequency offset (i.e., 1.7 ppm). In our experience with knee imaging, the B_0 inhomogeneity tends to be less than 0.5 ppm at 3T. To maintain high performance in fat suppression with the soft-hard composite pulse excitation, it is critical to have a system with a relatively uniform B_0 field and/or a high-performing shimming module

(e.g. high order shimming). Though fat suppression using the soft-hard pulse excitation is less uniform than the conventional FatSat module in this study, the image contrast between water and fat tissues with the soft-hard pulse excitation is still better than the FatSat images according to the calculated SSR values. The soft and hard pulses are two independent pulses in our soft-hard composite pulse implementation; thus, the center frequency of the soft pulse can be adjusted to account for B_0 inhomogeneity, if necessary. The proposed soft-hard pulse may be less sensitive to the B_1 inhomogeneity for fat suppression since the fat components always experience the same flip angles in opposite directions. The minimum phase pulse design can shorten the echo time, thus decreasing the T_2 decay during the soft pulse excitation. Then, the fat magnetization tipped down by the soft pulse can be largely tipped back by the hard pulse, thus allowing more efficient fat suppression.

Two groups have reported that the conventional binomial water excitation pulse provides excellent fat suppression with moderate short T_2 signal attenuations in UTE knee imaging (29,30). Similar simulations were performed in Springer's study (i.e., Fig. 4a) as in our study (i.e., Fig. 3) (29). Their simulation results demonstrated a stronger water attenuation with the binomial water excitation pulse when the tissue T_2s were getting shorter. However, our simulation results of the proposed soft-hard pulse excitation show a better performance in short T_2 tissue imaging, especially when the excitation flip angles are less than 10°. Our future studies are expected to compare the above three fat suppression techniques for quantitative UTE imaging, such as quantitative measures of T_1 (31,32), $T_{1\rho}$ (33,34), bi-component T_2^* analysis (35,36), MT ratio (MTR) (37), as well as MT modeling (38), which will provide more comprehensive understanding about the effect of different fat suppression schemes.

This study has several limitations. First, we have only demonstrated the technical feasibility of the proposed soft-hard composite pulse for fat suppression and water excitation in UTE imaging of both short and long T_2 tissues. No patients were studied in this work. Second, the proposed soft-hard pulse can only be used for non-selective 3D UTE imaging. A half-sinc pulse together with variable rate selective excitation (VERSE) may be used to replace the short rectangular pulse for slice/slab selective UTE imaging (39). Third, the effect of the soft-hard composite pulse on quantitative UTE imaging remains to be investigated.

Conclusion

The proposed soft-hard composite pulse is able to suppress fat signals while preserving both short and long T_2 signals, which is promising for both morphological and quantitative UTE imaging of short T_2 tissues.

Supplementary Material

Refer to Web version on PubMed Central for supplementary material.

Acknowledgments

References

1. Robson MD, Gatehouse PD, Bydder M, Bydder GM. Magnetic resonance: An introduction to ultrashort TE (UTE) imaging. J Comput Assist Tomogr 2003;27:825–846. [PubMed: 14600447]

2. Du J, Carl M, Bae WC, Statum S, Chang EY, Bydder GM, Chung CB. Dual inversion recovery ultrashort echo time (DIR-UTE) imaging and quantification of the zone of calcified cartilage (ZCC). Osteoarthritis Cartilage 2013;21(1):77–85. [PubMed: 23025927]

3. Chang EY, Du J, Bae WC, Chung CB. Qualitative and Quantitative Ultrashort Echo Time Imaging of Musculoskeletal Tissues. Semin Musculoskelet Radiol 2015;19(4):375–386. [PubMed: 26583365]

4. Du J, Carl M, Bydder M, Takahashi A, Chung CB, Bydder GM. Qualitative and quantitative ultrashort echo time (UTE) imaging of cortical bone. J Magn Reson 2010;207(2):304–11. [PubMed: 20980179]

5. Chen B, Cheng X, Dorthe EW, Zhao Y, D'Lima D, Bydder GM, Liu S, Du J, Ma YJ. Evaluation of normal cadaveric Achilles tendon and enthesis with ultrashort echo time (UTE) magnetic resonance imaging and indentation testing. NMR in Biomed 2018;20:e4034.

6. Wilhelm MJ, Ong HH, Wehrli SL, Li C, Tsai PH, Hackney DB, Wehrli FW. Direct magnetic resonance detection of myelin and prospects for quantitative imaging of myelin density. Proc Natl Acad Sci USA 2012;109:9605–9610. [PubMed: 22628562]

7. Sheth V, Shao H, Chen J, Vandenberg S, Corey-Bloom J. Bydder GM, Du J. Magnetic resonance imaging of myelin using ultrashort Echo time (UTE) pulse sequences: phantom, specimen, volunteer and multiple sclerosis patient studies. Neuroimage 2016;136:37–44. [PubMed: 27155128]

8. Gatehouse PD, Bydder GM. Magnetic resonance imaging of short T2 components in tissue. Clin Radiol 2003;58:1–19. [PubMed: 12565203]

9. Hennig J, Speck O. High-field MR imaging New York: Springer; 2011.

10. Del Grande F, Santini F, Herzka DA, Aro MR, Dean CW, Gold GE, Carrino JA. Fat-suppression techniques for 3-T MR imaging of the musculoskeletal system. Radiographics 2014;34(1):217–33. [PubMed: 24428292]

11. Carl M, Nazaran A, Bydder GM, Du J. Effects of fat saturation on short T2 quantification. Magn Reson Imaging 2017;43:6–9. [PubMed: 28629956]

12. Henkelman RM, Stanisz GJ, Graham SJ. Magnetization transfer in MRI: a review. NMR in Biomedicine 2001;14(2):57–64. [PubMed: 11320533]

13. Pauly JM, Conolly SM, Macovski A. Suppression of long T2 components for short T2 imaging. In: Proceedings of the 10th Annual Meeting of SMRI, New York, 1992 p 330.

14. Larson PE, Gurney PT, Nayak K, Gold GE, Pauly JM, Nishimura DG. Designing long-T2 suppression pulses for ultrashort echo time imaging. Magn Reson Med 2006;56(1):94–103. [PubMed: 16724304]

15. Larson PE, Conolly SM, Pauly JM, Nishimura DG. Using adiabatic inversion pulses for long-T2 suppression in ultrashort echo time (UTE) imaging. Magn Reson Med 2007;58:952–961. [PubMed: 17969119]

16. Du J, Takahashi AM, Bae WC, Chung CB, Bydder GM. Dual inversion recovery, ultrashort echo time (DIR UTE) imaging: Creating high contrast for short-T2 species. Magn Reson Med 2010;63(2):447–55. [PubMed: 20099332]

17. Carl M, Bydder GM, Du J. UTE imaging with simultaneous water and fat signal suppression using a time-efficient multispoke inversion recovery pulse sequence. Magn Reson Med 2016;76:577–582. [PubMed: 26309221]

18. Ma YJ, Zhu Y, Lu X, Carl M, Chang EY, Du J. Short T2 imaging using a 3D double adiabatic inversion recovery prepared ultrashort echo time cones (3D DIR-UTE-Cones) sequence. Magn Reson Med 2018;79(5):2555–63. [PubMed: 28913879]

19. Li S, Ma L, Chang EY, Shao H, Chen J, Chung CB, Bydder GM, Du J. Effects of inversion time on inversion recovery prepared ultrashort echo time (IR-UTE) imaging of bound and pore water in cortical bone. NMR in Biomed 2015;28(1):70–8.

20. Fan SJ, Ma Y, Zhu Y, Searleman A, Szeverenyi NM, Bydder GM, Du J. Yet more evidence that myelin protons can be directly imaged with Ute sequences on a clinical 3 T scanner: Bicomponent

analysis of native and deuterated ovine brain specimens. Magn Reson Med 2018;80(2):538–47. [PubMed: 29271083]

21. Jang H, Carl M, Ma Y, Jerban S, Guo T, Zhao W, Chang EY, Du J. Fat suppression for ultrashort echo time imaging using a single-point Dixon method. NMR in Biomedicine 2019 15:e4069.

22. Wang K, Yu H, Brittain JH, Reeder SB, Du J. k-space water-fat decomposition with T2* estimation and multifrequency fat spectrum modeling for ultrashort echo time imaging. J Magn Reson Imaging 2010;1;31(4):1027–34. [PubMed: 20373450]

23. Du J, Hamilton G, Takahashi A, Bydder M, Chung CB. Ultrashort echo time spectroscopic imaging (UTESI) of cortical bone. Magn Reson Med 2007;58(5):1001–9. [PubMed: 17969110]

24. Pauly JM, Le Roux P, Nishimura DG, Macovski A. Parameter relations for the Shinnar-Le Roux selective excitation pulse design algorithm. IEEE Trans Med Imaging 1991;10:53–65. [PubMed: 18222800]

25. Jerban S, Ma Y, Nazaran A, et al. Detecting stress injury (fatigue fracture) in fibular cortical bone using quantitative ultrashort echo time-magnetization transfer (UTE-MT): An ex vivo study. NMR Biomed 2018;31:e3994. [PubMed: 30059184]

26. Jerban S, Ma Y, Wong JH, Nazaran A, Searleman A, Wan L, Williams J, Du J, Chang EY. Ultrashort echo time magnetic resonance imaging (UTE-MRI) of cortical bone correlates well with histomorphometric assessment of bone microstructure. Bone 2019;123:8–17. [PubMed: 30877070]

27. Jerban S, Ma Y, Wan L, Searleman AC, Jang H, Sah RL, Chang EY, Du J. Collagen proton fraction from ultrashort echo time magnetization transfer (UTE-MT) MRI modelling correlates significantly with cortical bone porosity measured with micro-computed tomography (µCT). NMR Biomed 2019;32:1–10.

28. Lu X, Jerban S, Wan L, Ma Y, Jang H, Le N, Yang W, Chang EY, Du J. Three Dimensional Ultrashort Echo Time Imaging with Tri-component Analysis for Human Cortical Bone. Magn. Reson. Med 2019;82:348–355. [PubMed: 30847989]

29. Springer F, Steidle G, Martirosian P, Grosse U, Syha R, Schabel C, Claussen CD, Schick F. Quick water-selective excitation of fast relaxing tissues with 3D UTE sequences. Magn Reson Med 2014;71(2):534–43. [PubMed: 23440968]

30. Deligianni X, Bär P, Scheffler K, Trattnig S, Bieri O. Water-selective excitation of short T2 species with binomial pulses. Magn Reson Med 2014;72(3):800–5. [PubMed: 24123175]

31. Ma YJ, Lu X, Carl M, Zhu Y, Szeverenyi NM, Bydder GM, Chang EY, Du J. Accurate T1 mapping of short T2 tissues using a three-dimensional ultrashort echo time cones actual flip angle imaging variable repetition time (3D UTE-Cones AFI-VTR) method. Magn Reson Med 2018;80(2):598–608. [PubMed: 29314235]

32. Ma YJ, Zhao W, Wan L, Guo T, Searleman A, Jang H, Chang EY, Du J. Whole Knee Joint T1 Values Measured In Vivo at 3T by Combined 3D Ultrashort Echo Time Cones Actual Flip Angle and Variable Flip Angle Method. Magn Reson Med 2018;DOI: 10.1002/mrm.27510.

33. Du J, Carl M, Diaz E, Takahashi A, Han E, Szeverenyi NM, Chung CB, Bydder GM. Ultrashort TE T1rho (UTE-T1rho) imaging of the Achilles tendon and meniscus. Magn Reson Med 2010;64(3):834–842. [PubMed: 20535810]

34. Ma YJ, Carl M, Searleman A, Lu X, Chang EY, Du J. 3D adiabatic T1ρ prepared ultrashort echo time cones sequence for whole knee imaging. Magn Reson Med 2018;80:1429–1439. [PubMed: 29493004]

35. Du J, Diaz E, Carl M, Bae W, Chung CB, Bydder GM. Ultrashort echo time imaging with bicomponent analysis. Magn Reson Med 2012;67(3):645–9. [PubMed: 22034242]

36. Seifert AC, Wehrli SL, Wehrli FW. Bi-component T2* analysis of bound and pore bone water fractions fails at high field strengths. NMR in Biomed 2015;28(7):861–72.

37. Grosse U, Syha R, Martirosian P, Wuerslin C, Horger M, Grozinger G, €Schick F, Springer F. Ultrashort echo time MR imaging with offresonance saturation for characterization of pathologically altered Achilles tendons at 3 T. Magn Reson Med 2013;70:184–192 [PubMed: 22851408]

38. Ma YJ, Shao H, Du J, Chang EY. Ultrashort echo time magnetization transfer (UTE-MT) imaging and modeling: magic angle independent biomarkers of tissue properties. NMR in Biomed 2016;29(11):1546–52.

39. Hargreaves BA, Cunningham CH, Nishimura DG, Conolly SM. Variable-Rate Selective Excitation for Rapid MRI Sequences. Magn Reson Med 2004;52:590–597. [PubMed: 15334579]
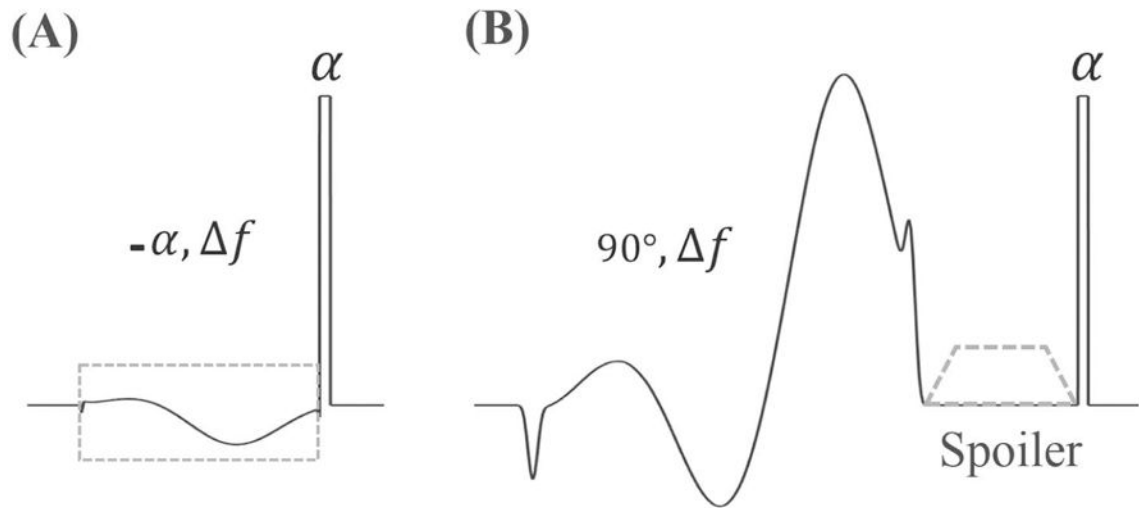
Figure 1.
The proposed soft-hard composite pulse (A) and the conventional FatSat module (B). A soft RF pulse centered on fat on-resonance frequency (f) with a negative flip angle (−α) was used to flip the fat magnetization only, followed by a short hard pulse with a positive flip angle (α) to flip all the magnetizations in the opposite direction (A). The commonly used FatSat module is shown in (B) for comparison. A 90° soft pulse centered on fat on-resonance frequency was used to flip down the fat magnetization and then all the excited transverse magnetizations were crushed by a gradient spoiler. A following hard pulse was used for water signal excitation. The RF phases of soft pulses in A and B were determined by their center frequencies.
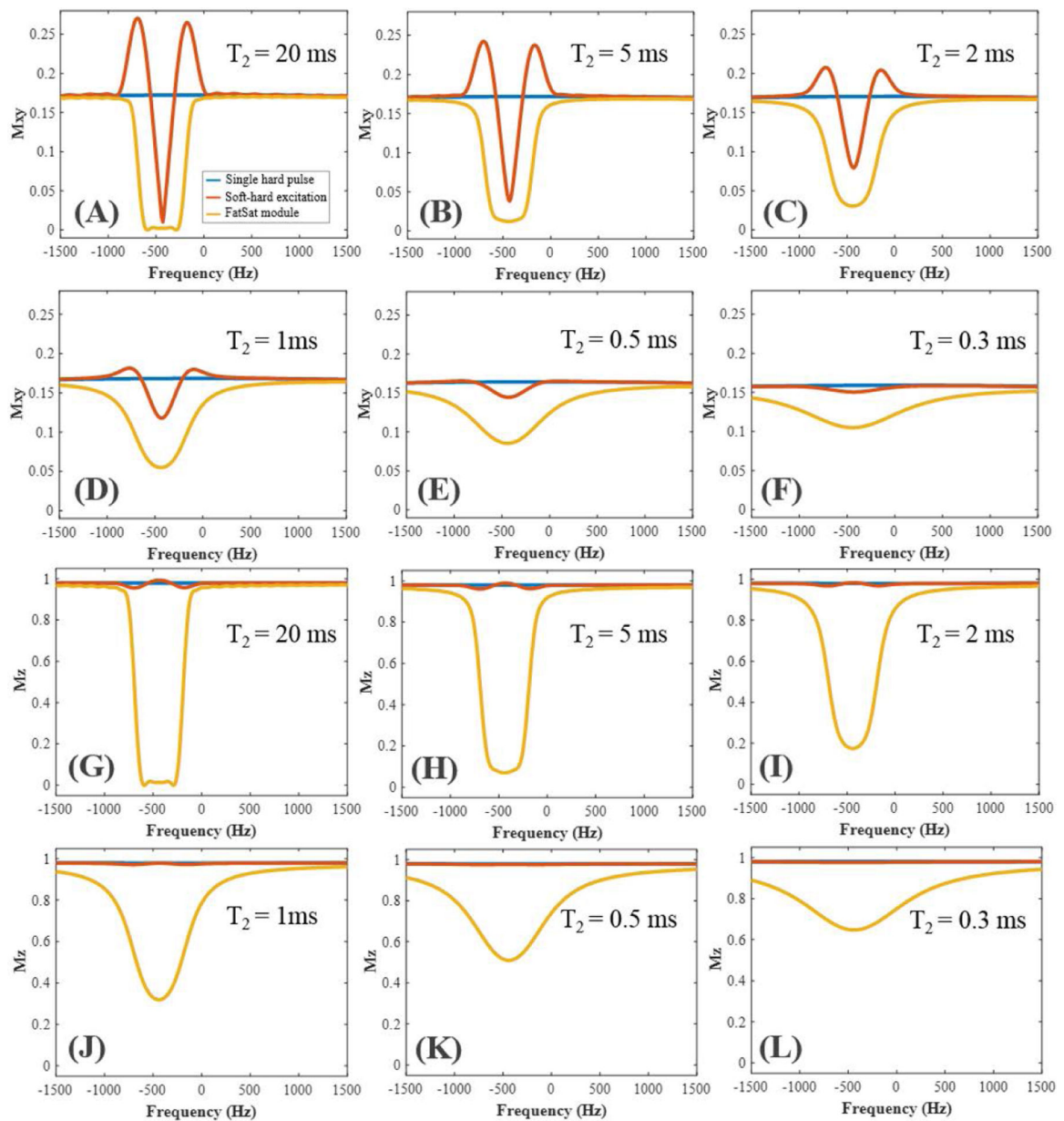
Figure 2.
Bloch simulations for the excitations of a single hard pulse (blue curves), the proposed soft-hard composite pulse (red curves), and the conventional FatSat module (yellow curves). Both transverse (A–F) and longitudinal (G–L) magnetization profiles were calculated for tissues with different T_2s of 20, 5, 2, 1, 0.5, and 0.3 ms. Much lower saturation effect was observed for the proposed soft-hard composite pulse compared with that of the FatSat module.
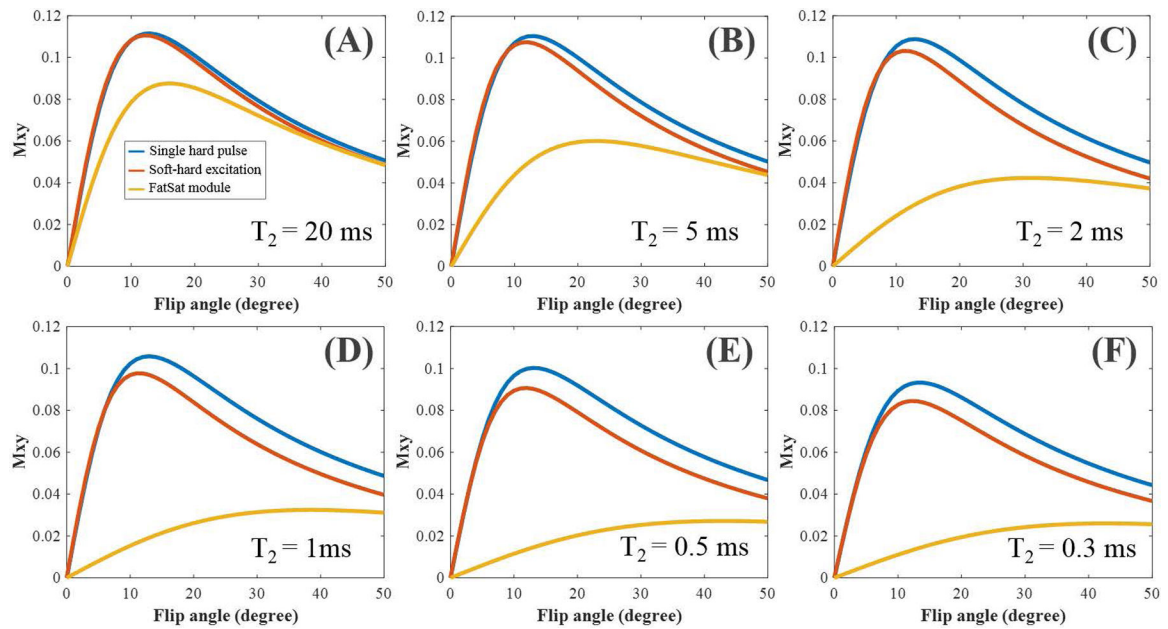
Figure 3.
Simulations of UTE imaging using the excitations with a single hard pulse (blue curves), the proposed soft-hard composite pulse (red curves), and the conventional FatSat module (yellow curves), respectively. The UTE signal intensities changed with the flip angles ranged from 0° to 50°. Six different T_2s of 20, 5, 2, 1, 0.5, and 0.3 ms were used to simulate both long and short T_2 tissues. All the tissue T_1s were set to a constant value of 800 ms for simulation.
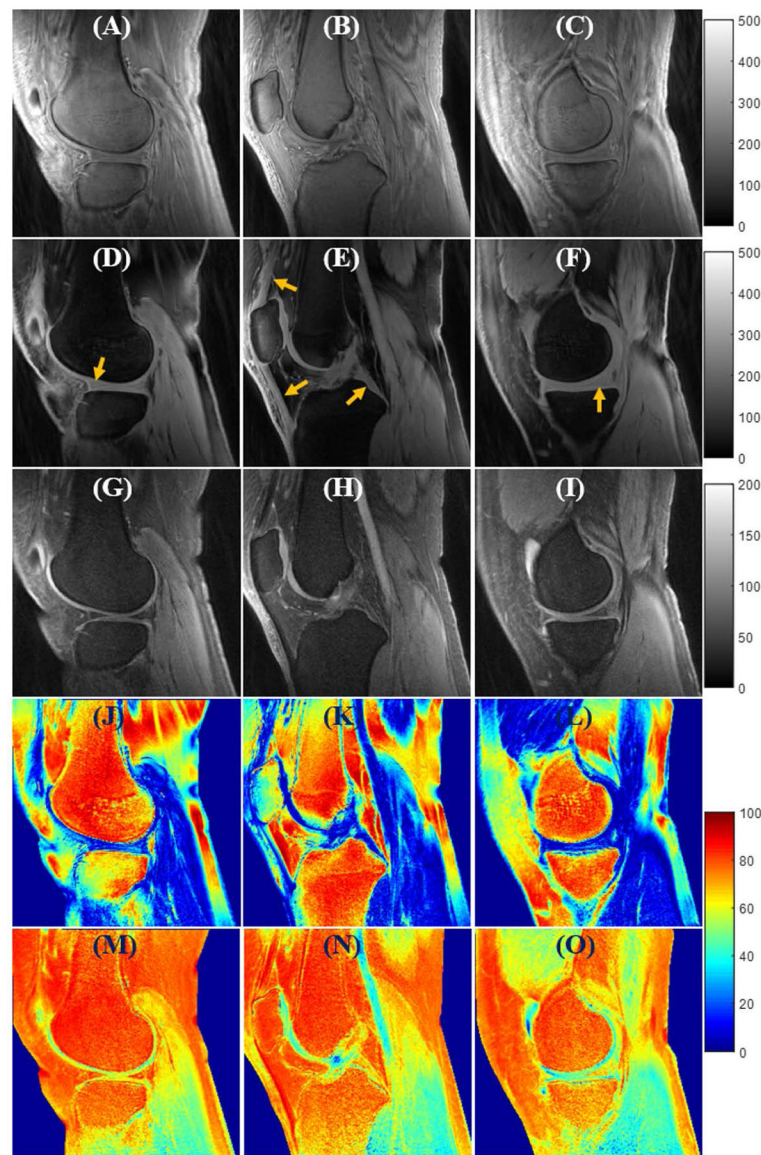
Figure 4.
In vivo knee joint UTE-Cones imaging (from a 24-year-old volunteer) using excitations with a single hard pulse (A–C), the proposed soft-hard water excitation pulse (D–F), and the conventional FatSat module (G–I). Fat was well suppressed by both the proposed soft-hard pulse and the FatSat module. The short T_2 signals (indicated by yellow arrows in D–F) were much better preserved in the soft-hard excitation images (D–F) compared with FatSat images (G–I). The SSR colormaps (soft-hard pulse: J–L; FatSat module: M–O) also suggest that there were almost no signal attenuations for either short or long T_2 tissues when using the proposed soft-hard pulse for excitation. In comparison, there were strong signal attenuations for the water signals in the FatSat UTE-Cones images, especially for the short T_2 tissues.
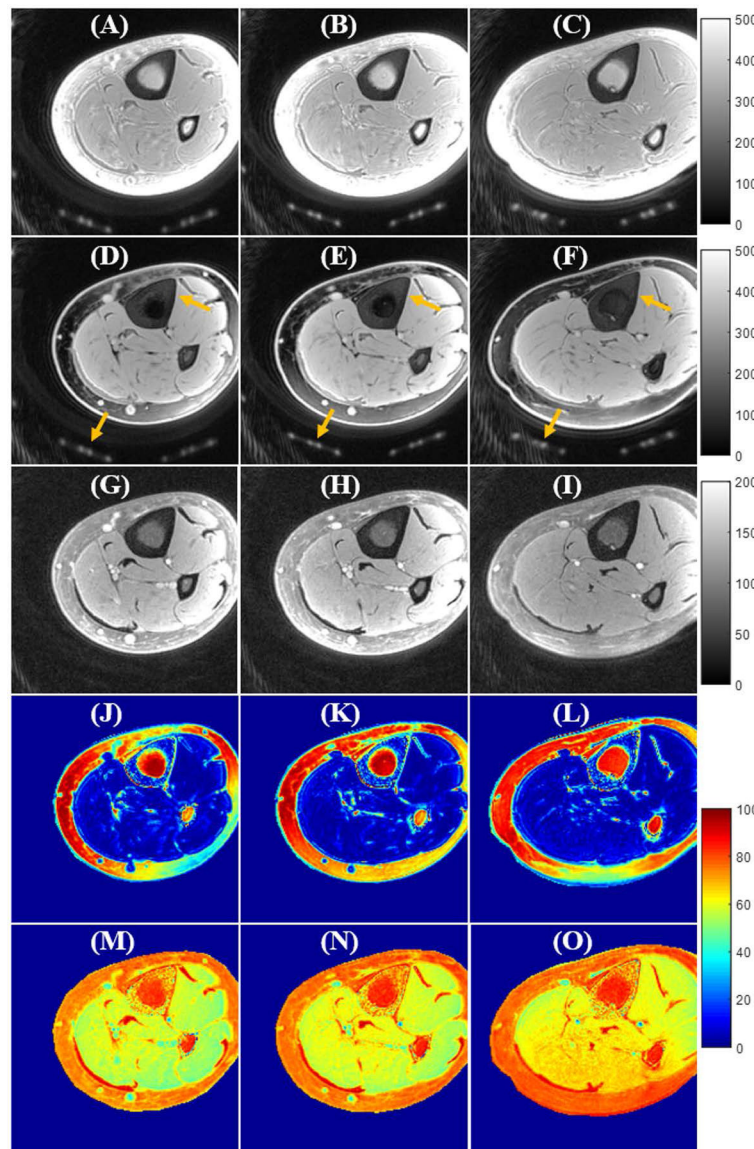
Figure 5.
In vivo tibia UTE-Cones imaging (from a 35-year-old volunteer) using excitations with a single hard pulse (A–C), the proposed soft-hard water excitation pulse (D–F), and the conventional FatSat module (G–I). Fat was well suppressed by both the proposed soft-hard pulse and the FatSat module. The cortical bone and coil elements (indicated by yellow arrows in D–F) were much better preserved in the soft-hard excitation images (D–F) compared with FatSat images (G–I). The SSR colormaps (soft-hard pulse: J–L; FatSat module: M–O) also suggest that there were almost no signal attenuations for either short or long T_2 tissues when using the proposed soft-hard pulse for excitation. In comparison, there were strong signal attenuations for the water signals in the FatSat UTE-Cones images, especially for the short T_2 tissues.